# Mechanism of a Soluble Fumarate Reductase from *Shewanella frigidimarina*: A Theoretical Study

**M. Fátima Lucas and Maria J. Ramos***

*REQUIMTE, Departamento de Química, Faculdade de Ciências da Universidade do Porto, Rua do Campo Alegre, 687, 4169-007 Porto, Portugal*

*Received: December 22, 2005; In Final Form: March 10, 2006*

The mechanism of a unique fumarate reductase is explored using the hybrid density functional B3LYP method. The calculations show a two-step mechanism, initiated with a hydride transfer from FAD (flavin adenine dinucleotide) to fumarate, followed by a proton shift from Arg402. The rate-limiting process is assigned to the hydride transfer, and the energetics are consistent with experimental data. It is shown that the enzyme is essential to correctly position the substrate in the active site, stabilizing its extremely anionic character.

## Introduction

In mitochondrial aerobic respiration, electrons are transferred along a series of membrane-bound protein complexes (I, II, III, and IV; see Figure 1), known as the electron transport chain, to oxygen as the terminal electron acceptor.[1−3] Complex II, which is frequently referred to as succinate dehydrogenase, has a dual function and is also responsible for catalyzing the oxidation of succinate into fumarate as part of the Krebs cycle.[4]

During the oxidation of succinate, two electrons and two protons are produced and the flavin adenine dinucleotide (FAD) cofactor of the enzyme succinate dehydrogenase is reduced. The electrons are then transferred to quinone, a hydrophobic membrane bound carrier which is reduced to quinol, and for this reason complex II is more correctly named succinate: quinone reductase (SQR).[5,6] However, in the absence of oxygen, many microorganisms are able to obtain energy through anaerobic respiratory processes using alternate electron acceptors.[7,8] One of the most frequently used is fumarate that is reduced to succinate by quinol:fumarate reductase (QFR).[9−11] The importance of QFR can be understood if we consider that not only does it enable bacteria to respire in the absence of oxygen but also it is similar in structure and function to SQR, and is able to functionally replace this enzyme in aerobic respiration when conditions allow it to be expressed anaerobically.[12] SQR and QFR complexes are anchored in the cytoplasmatic membranes of eubacteria such as *Escherichia coli*[9,13−15] and *Wolinella succinogenes*[16] and in the inner mitochondrial membrane of eukaryotes.[17−19] Recently there has been reference to some soluble, periplasmatic, fumarate reductase belonging to *Shewanella* species.[20−23] It is known that some facultative anaerobes, such as *Escherichia coli*, are able to reversibly oxidize succinate.[24−26] Kinetic experiments on *Escherichia coli* SQR have shown that although the enzyme is capable of both reactions it is more proficient in oxidizing succinate than reducing fumarate at a rate of 40:1.[27] However, the efficiency of the enzyme in both directions is dependent on the applied potential and pH.[28] In recent years a significant number of high-resolution X-ray structures of complex II from *Escherichia coli*,[14,29,30] *Wolinella succinogenes*,[16,31] and *Shewanella* species[20−23] have become available that show significant similarities in their active sites, suggesting that the anaerobic and aerobic forms of complex II must have a common evolutionary precursor.[5,7,32,33] Despite these similarities, the soluble, tetraheme flavocytochrome $c_3$[21] found in *Shewanella* species presents considerable differences, containing a noncovalently bound FAD, opposed to the 8α-(N3)-histidyl-FAD encountered in membrane-bound enzymes.[34] Some site directed mutagenesis studies on *Escherichia coli*[35] and *Saccharomyces cerevisiae*[36] where the FAD group was unable to covalently bond to the enzyme show that the enzymes are incapable of oxidizing succinate. This important

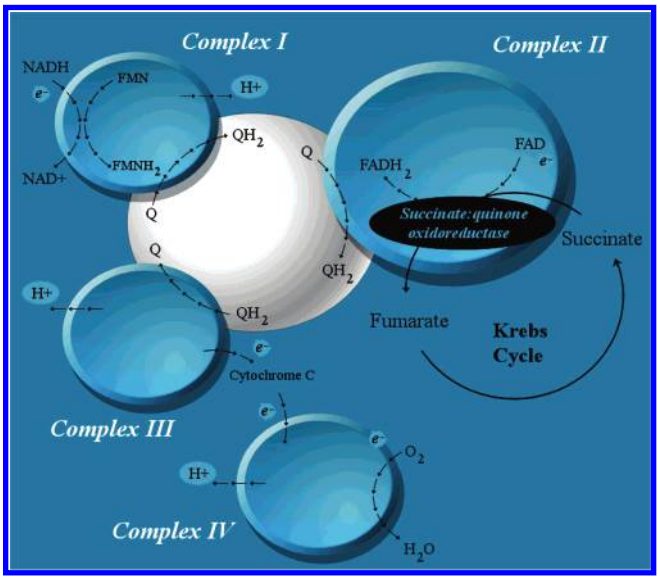


**Figure 1.** Simplified schematic representation of the mitochondrial aerobic respiratory chain. Complex I, also known as NADH (nicotinamide adenine dinucleotide):ubiquinone oxidoreductase, catalyzes electron transfer from NADH to quinone (Q), which is reduced to quinol ($QH_2$) through a series of redox centers that include a flavin mononucleotide (FMN) moiety and an iron−sulfur cluster. The flow of electrons from NADH to $QH_2$ leads to the production of four $H^+$ ions. $FADH_2$ is formed in the Krebs cycle during the oxidation of succinate to fumarate by succinate dehydrogenase—complex II. Electrons are then transferred from $FADH_2$ through an Fe−S cluster to quinone. The function of complex III (ubiquinone:cytochrome *c* oxidoreductase) is to catalyze the transfer of electrons from $QH_2$ to cytochrome *c*. Complex IV accepts electrons from cytochrome *c* and passes them to oxygen.

* Corresponding author. E-mail: mjramos@fc.up.pt.

10.1021/jp057456t CCC: $33.50 
Published on Web 05/06/2006

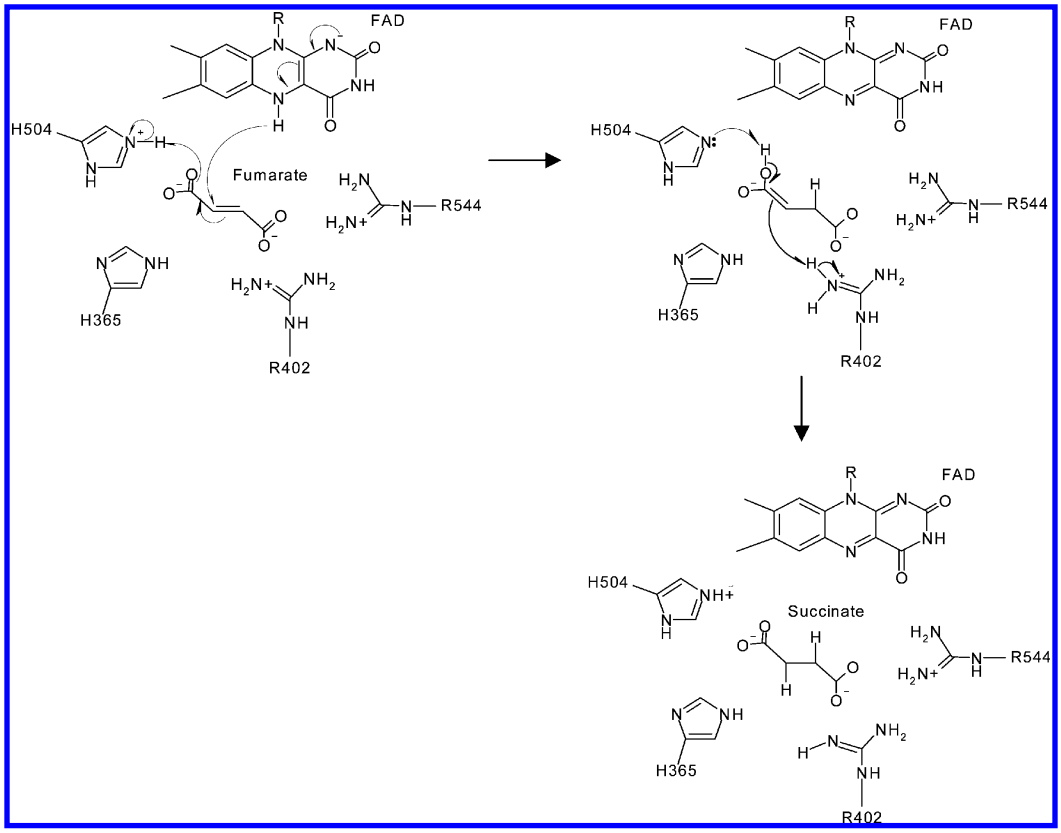


**Figure 2.** Schematic representation of the reaction mechanism for fumarate reductase as proposed by Taylor et al.[21]

feature is encountered in the soluble QFR and constitutes a major distinction.[37,38]

In this work we aim to study the mechanism of a soluble fumarate reductase from *Shewanella frigidimarina* and help clear some aspects in the path of fumarate reduction. There has been intense experimental work[14,16,22,23,31,39,40] through the years on the mechanism of fumarate reductases, and previous studies[21,22,39] predict that the reaction is initiated by the polarization of the substrate, as a result of interactions with the charged residues in the active site, which facilitates the hydride transfer from the reduced flavin adenine dinucleotide. The experimentally based mechanism[21] is shown in Figure 2, which also illustrates His504 protonating the C4 carboxylate to facilitate the transient formation of a carbanion in the substrate. The reaction should then proceed with a proton transfer, and several residues have been proposed for this function.[13,16,41] A recent study has unequivocally assigned the proton transfer to Arg402. It has been shown that the R402A mutant enzyme is completely inactive under all conditions,[22] and inspection of the X-ray structure of the wild-type enzyme shows that Arg402 is ideally positioned for proton donation.[39,42]

## Computational Details

All geometries involved in the reaction studied were optimized using density functional theory (DFT) as implemented in Gaussian03[43] quantum chemistry packages. The combination of Becke's three parameter hybrid function[44−47] with the Lee−Yang−Parr correlation functional[48] (B3LYP) was used with a double $\xi$ basis set on all atoms (6-31G(d)). The same level of theory was used to characterize all stationary points by determination of the Hessian. The Hessian was also employed to estimate zero-point, thermal, and entropy effects in the relative energies. We must add a note on the values of $\Delta G$ presented in this work. Frequency calculations are valid only at stationary points on the potential energy surface. Therefore, frequency calculations should be performed on fully optimized structures, i.e., with no constraints imposed on atomic positions. However, in small truncated models of enzymatic systems, it is often necessary to constrain the truncated atoms to their crystallographic positions whenever severe drifting from the residues occurs. This means that the transition state (TS) that we calculated cannot be fully optimized and accordingly frequency calculations should not take place. However, experience has shown that usually when we do so, in most enzymatic systems, the TS even though not characterized by one imaginary frequency only, has associated very small values for the other imaginary frequencies. The calculated thermal corrections are in any case very small, and the respective entropic contributions do not alter significantly the energy barriers obtained.[49−55] Therefore, we warn the reader that the values of $\Delta G$ presented here are an approximation to the real values that we would obtain were we able to freely optimize our model. The final B3LYP energies for the optimized structures were evaluated performing a single-point calculation using the 6-311++G(3df, 3p) basis, with polarized and diffuse functions added to all atoms. The dielectric effect from the surrounding environment, which accounts for the protein and the buried water molecules, was obtained using the C-PCM polarizable conductor model (Cosmo) developed by Barone and Cossi.[56−63] The dielectric constant was set to 4, which has been shown to be in agreement with experimental results.[50,64−67] The relative energies discussed below are Gibbs energies with solvent effects included.

## Chemical Models

When the study of an enzyme is considered, by means of quantum chemistry, the first point in which we must concentrate is the appropriate choice of a model for the active site and the substrate. In this work, we have used the crystal structure of

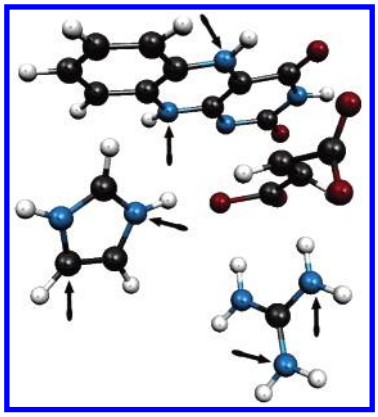

**Figure 3.** Model of the enzyme active site. This system contains the exact positions as found in the crystal structure. Fumarate, however, has been obtained by direct substitution of the malate-like molecule found in the crystallographic file, by the appropriate substrate.

flavocytochrome $c_3$ from *Shewanella frigidimarina* (PDB entry 1qjd) with a 1.8 Å resolution.[21] The analysis of the crystal structures of fumarate reductases from different species (*Escherichia coli*, *Wolinella succinogenes*, and *Shewanella* species) indicate that all amino acid residues involved in substrate binding and catalysis are conserved, which is consistent with the possibility of a common mechanism for this family of enzymes.[22] It is generally agreed that a flavin adenine dinucleotide binding domain is responsible for the hydride transfer. However, the source of the proton donor has been the subject of discussion over the years.[13,16,41] Recently, a mutagenesis study involving His365, His504, and Arg402 has revealed that Arg402 is the most probable proton donor.[22] The size of the system to be used is limited by the computational effort involved, and to find the best compromise that simultaneously describes, in a correct manner, the biological behavior of the enzyme in a realistic time frame, several tests have been performed. Two models have been considered, one composed of a restricted FAD model (as shown in Figure 3), fumarate, Arg402, and His504, and a larger model where His 365 and Arg544 have also been added. We have observed that no changes took place in the systems' behavior with the larger model, which led us to adopt for all studies the smaller system given the minor computational effort.

The selected model contains 53 atoms that represent fragments of the residues essential for substrate binding and catalysis. To introduce a certain degree of protein strain, a few nuclear positions were fixed during the geometry optimization, and to keep all residues close to the crystal structure, we have employed a frame model. In this model, we strategically kept some atoms frozen to ensure that the system contained the exact positions as found in the protein. The model employed, observed in Figure 3, included the FAD and the side chains of His504 and Arg402 as found in the crystallographic file and the fumarate which was obtained by direct substitution from the malate-like molecule.

The energetics for this reaction and all pertinent structures were established using this model; however, as predicted by experimental studies, the substrate must be stabilized by the surrounding residues included in the active site. Therefore, it was necessary to compensate the anionic character of the substrate, and instead of fumarate, fumaric acid was used. It should be noted that the use of neutral models to reproduce highly charged systems has been customary through the years to prevent unrealistic behavior in the gas phase and diminish convergence problems.[68−70] In this work, however, the use of a neutral model for the substrate has been the result of a careful analysis of the system and is not related to technical problems. The carboxylate moiety is included in a center with strong hydrogen bonds to positively charged groups, such as arginines. To keep the computational cost to a minimum, it was not possible to include a large enough number of residues to compensate the considerable charge concentration involved in this system, and for this reason the use of fumaric acid leads to more accurate results, despite a total charge of +1 for the model employed.

## Results

**Reaction Sequence.** We have referred beforehand to the fact that the conversion of fumarate into succinate is expected to take place, first with a hydride transfer from FAD followed by a proton shift from Arg402 to fumarate. This section describes all aspects of the reaction path.

**Hydride Transfer.** The first step in the catalytic reaction of fumarate reductase is a hydride transfer from N5 of the reduced FAD group to the substrate; all pertinent structures can be observed in Figure 4.

This step is accompanied by an activation energy of 17.0 kcal mol$^{-1}$, and the product lies 3.0 kcal mol$^{-1}$ below the reagent's energy. It can also be seen, as expected,[11] that the normally planar substrate in the reagent has lost planarity upon interaction with the enzyme. This effect should facilitate the nucleophilic attack on C2 by destabilizing the double bond, which is slightly elongated. We have also observed that the position of the substrate relative to FAD is a main factor in this step. Close examination of the system has revealed that the activation barrier is directly dependent on the distance between the hydride atom on FAD and the substrate C2 atom, and even a slight increase leads to significant rise in energy. Based on the observation of several crystallographic files of this enzyme, we have restrained the distance between the hydrogen N5 on FAD and the substrate to correctly reproduce the natural behavior of the system, avoiding deviations not possible in the enzyme. We have also observed that the study of this step using charged models has revealed that the presence of a protonated histidine residue in the active site leads to a different mechanistic path. Experimentally based studies have proposed that throughout the reaction, and to facilitate the hydride transfer from the reduced flavin adenine dinucleotide, it is possible that a proton transfer occurs from a neighboring histidine to fumarate's carboxylate moiety. However, these proposals have always referred to this as taking place following the hydride transfer. All studies using charged models have shown a consistent proton transfer previous to the hydride transfer and no barrier has been observed; i.e., once the system is optimized in the search for the transition state involving the hydride transfer, the proton on the histidine is spontaneously shifted to the fumarate carboxylate group. This will be further discussed at a later stage.

**Proton Transfer from Arginine-402.** The next step in the proposed mechanism is the proton transfer from Arg402 to the substrate C3 atom with consequent succinate production. The barrier was established to be 4.2 kcal mol$^{-1}$, and the step is exothermic by 6.3 kcal mol$^{-1}$. All structures are shown in Figure 5.

## Discussion

It was found that the rate-limiting step of the proposed mechanism is the hydride transfer with an activation barrier of 17.0 kcal mol$^{-1}$. This barrier reproduces very well the experi-

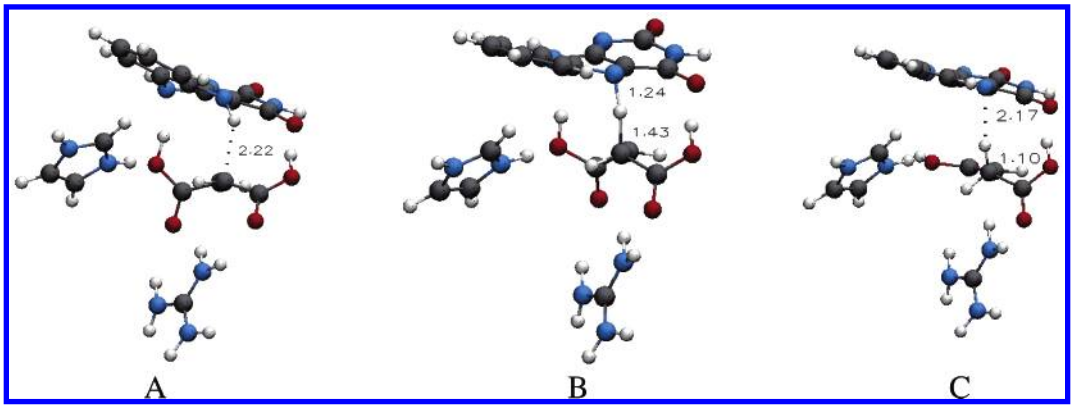


**Figure 4.** Optimized structures for step 1, the hydride transfer from N5 of the reduced FAD to the substrate C2 atom: (A) reactant; (B) transition state; (C) product. Important distances are given in angstroms.

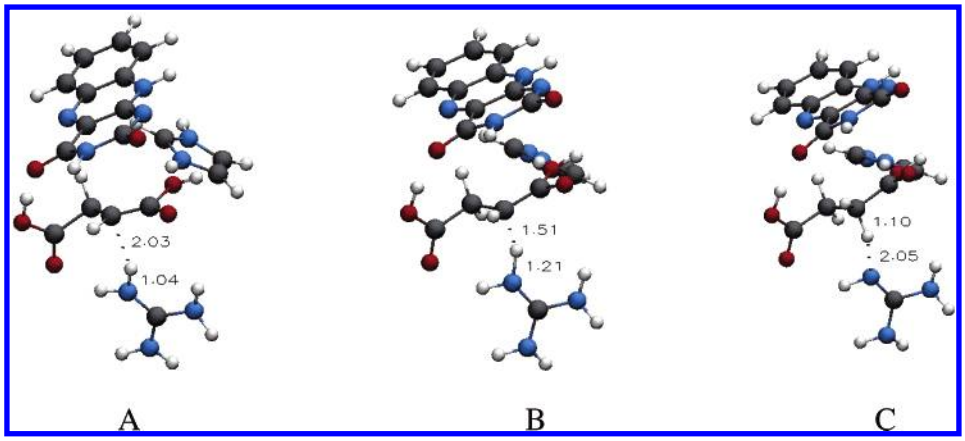


**Figure 5.** Optimized structures for step 2, the proton transfer from Arg402 to the substrate C3 atom: (A) reactant; (B) transition state; (C) product. Important distances are given in angstroms. Please note that, although in a different spatial orientation (for a better observation of the pertinent distances), (A) has the same geometry as Figure 4C.

mental data[38] for the turnover rate with $k_{cat} = 509\ s^{-1}$ at 25 °C and pH 7.2, corresponding to a rate-limiting barrier of approximately 14 kcal $mol^{-1}$. Even though the calculated barrier is somewhat higher than the experimental limit, the discrepancy is within the normal error of 3−5 kcal $mol^{-1}$ for the computational method used. The overall reaction is accompanied by an exothermicity of 9 kcal $mol^{-1}$.

Site directed mutagenesis studies have discarded His504 as the possible proton donor for the second step of this reaction.[22] However, it is known to have an important function in this mechanism. We have performed several studies with two systems and observed that the His504 can have a direct influence on the mechanistic path, but the inclusion of any other residues, namely the positively charged Arg544 or His365, has no effect on the energy barrier. We have observed that whenever the carboxylate group in the vicinity of His504 is unprotonated, the reaction takes place with an unexpected proton transfer from His504 to fumarate's anionic carboxylate group at the very beginning of the reaction. This was observed in all studies (except when fumaric acid was used), and is opposed to what was proposed experimentally,[21] where this was predicted to take place following the hydride transfer. To establish unequivocally this aspect of the reaction, it would be necessary to use a very large model, including the entire enzyme or a large enough number of residues, to neutralize the charge concentration observed in the active site; this study is in development for future insight in the enzyme. In the studies we have conducted here, we observed that if the proton is to be shifted this will occur at the beginning of the reaction with little or no activation barrier. In addition to this effect we have observed that the protonation

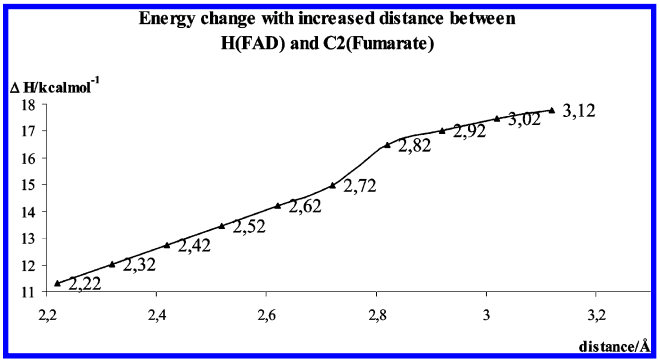


**Figure 6.** Observed energy variation with distance between hydrogen atom on FAD and C2 atom on fumarate.

of the terminal carboxylate groups of fumarate lowers, i.e., compensating for a high concentration of charge, the activation barrier by about 20%. It is clear that the enzyme has a critical effect in lowering the energy barrier, and we expect that the stabilization should occur mainly on the transition state given its highly anionic character. It is clear from these results that other factors, for instance residues responsible for stereochemical orientation, and not only the residues involved in catalysis, have an unquestionable influence in achieving a lowered activation barrier.

In addition to the stabilizing effect of the protein on the substrate, we have also noticed that the distance between the hydride atom on FAD and the substrate has a direct influence on the activation barrier for this reaction. We have performed a potential energy scan between the C2 carbon atom on fumarate and the hydrogen atom in FAD and observed that there is a

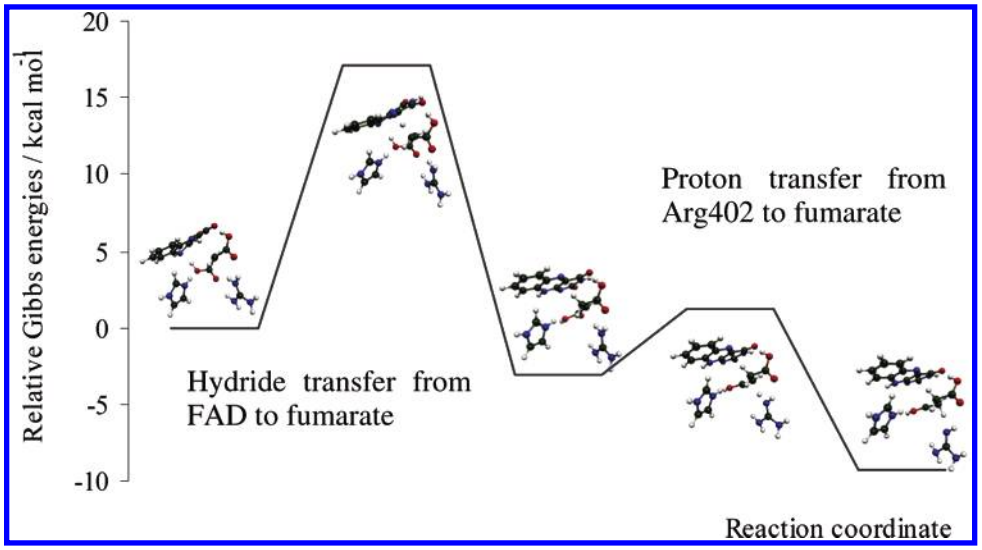


**Figure 7.** Calculated potential energy surface and optimized structures for fumarate reduction by fumarate reductase.

direct connection between their distance and the energetic barrier to be surmounted. The energy scan can be observed in Figure 6.

For the reaction to take place, it is essential that the substrate is correctly positioned in the active center, since increasing the distance increases the barrier proportionally. Observation of a significant number of crystallographic structures of this enzyme shows that the distance between the hydrogen atom in the FAD molecule and C2 on fumarate is essentially maintained. We have established that the rate of the reaction depends on the stabilization of the substrate as well as the distance between the C2 carbon atom on fumarate and the hydride from the FAD molecule.

All optimized structures and the calculated potential energy surface for the full reaction are presented in Figure 7. Energies shown were evaluated at the 6-311++G(3df, 2p) level with zero-point, thermal, and entropy effects calculated with the 6-31G(d) basis set, and the C-PCM polarizable continuum was included to model the protein surroundings.

## Conclusion

We present here the first theoretical approach toward studying the catalytic mechanism of a unique fumarate reductase. The reaction has been investigated using B3LYP hybrid DFT method, and the models used were based on the X-ray structure of flavocytochrome $c_3$ from *Shewanella frigidimarina* with a 1.8 Å resolution.

We were able to determine the energy profile for the reaction, two transition states were optimized, and their nature was confirmed by frequency analysis using the B3LYP functional at the 6-31G(d) level. We have confirmed that hydride transfer from the N5 on the reduced FAD molecule, followed by a proton shift from the neighboring Arg402, provides an energetically reasonable mechanism.

It has been established that there is a possible alternate route for the mechanism that includes a proton shift from His504 to the neighboring carboxylate group in fumarate, which we could not establish unequivocally with the model used here; however, if this transfer is to take place, it will occur at the beginning of the reaction, and not following the hydride transfer as proposed previously.

We were able to establish the rate-limiting process to be the hydride transfer from the FAD molecule, evidence the importance of the enzyme in lowering the activation barrier, by stabilizing the extremely anionic substrate as well as positioning it correctly in the active site, and present the prospect of a new mechanistic pathway. This information promotes new possibilities for future experimental and theoretical work in this important field of research.

**Acknowledgment.** The authors acknowledge Prof. Malcolm Walkinshaw for the invitation to work on the Shewanella Fumarate Reductase project and for a critical review of the information presented here. The Fundação para a Ciência e Tecnologia (Ph.D. grant for M.F.L.) is gratefully acknowledged, as is the support of the European Commission through Grant HPRI-CT-1999-00026 (the TRACS Programme at EPCC).

**Supporting Information Available:** PDB files of all optimized structures: structure 1; structure 2; structure 3; structure 4; structure 5. This material is available free of charge via the Internet at http://pubs.acs.org.

## References and Notes

(1) Keilin, D. On cytochrome, a respiratory pigment common to animal, yeast, and higher plants. *Proc. R. Soc.* **1925**, *98*, 312−339.

(2) Mitchell, P. Keilin's respiratory chain concept and its chemiosmotic consequences. *Science* **1979**, *206* (4423), 1148−1159.

(3) Saraste, M. Oxidative phosphorylation at the fin de siecle. *Science* **1999**, *283* (5407), 1488−1493.

(4) Krebs, H. A.; Johnson, W. A. The role of citric acid in intermediate metabolism in animal tissues. *Enzymologia* **1937**, *4*, 148−156.

(5) Hagerhall, C. Succinate:quinone oxidoreductases. Variations on a conserved theme. *Biochim. Biophys. Acta* **1997**, *1320*, 107−141.

(6) Lancaster, C. R. D. Succinate:quinone oxidoreductases: an overview. *Biochim. Biophys. Acta* **2002**, *1553* (1−2), 1−6.

(7) Hederstedt, L. Respiration Without O2. *Science* **1999**, *284* (5422), 1941−1942.

(8) Newman, D. K. Microbiology: How bacteria respire minerals. *Science* **2001**, *292* (5520), 1312−1313.

(9) Kröger, A. Fumarate as terminal acceptor of phosphorylative electron transport. *Biochim. Biophys. Acta* **1978**, *505* (2), 129−145.

(10) Kröger, A.; Geisler, V.; Lemma, E.; Theis, F.; Lenger, R. Bacterial fumarate respiration. *Arch. Microbiol.* **1992**, *158*, 311−314.

(11) Reid, G. A.; Miles, C. S.; Moysey, R. K.; Pankhurst, K. L.; Chapman, S. K. Catalysis in fumarate reductase. *Biochim. Biophys. Acta* **2000**, *1459* (2−3), 310−315.

(12) Maklashina, E.; Berthold, D. A.; Cecchini, G. Anaerobic Expression of Escherichia coli Succinate Dehydrogenase: Functional Replacement of Fumarate Reductase in the Respiratory Chain during Anaerobic Growth. *J. Bacteriol.* **1998**, *180* (22), 5989−5996.

(13) Schröder, I.; Gunsalus, R. P.; Ackrell, B. A. C.; Cochran, B.; Cecchini, G. Identification of active site residues of Escherichia coli fumarate reductase by site-directed mutagenesis. *J. Biol. Chem.* **1991**, *266*, 13572−13579.

(14) Iverson, T. M.; Luna-Chavez, C.; Cecchini, G.; Rees, D. C. Structure of the Escherichia coli fumarate reductase respiratory complex. *Science* **1999**, *284*, 1961−1966.

(15) Cecchini, G.; Schröder, I.; Gunsalus, R. P.; Maklashina, E. Succinate dehydrogenase and fumarate reductase from Escherichia coli. *Biochim. Biophys. Acta* **2002**, *1553* (1−2), 140−157.

(16) Lancaster, C. R. D.; Kroger, A.; Auer, M.; Michel, H. Structure of fumarate reductase from Wolinella succinogenes at 2.2 Å resolution. *Nature* **1999**, *402*, 377−385.

(17) Singer, T. P.; Kearney, E. B.; Kenney, W. C. Succinate dehydrogenase. *Adv. Enzymol.* **1973**, *37*, 189−272.

(18) Hederstedt, L.; Rutberg, L. Succinate Dehydrogenase−a Comparative Review. *Microbiol. Rev.* **1981**, *45*, 542−555.

(19) Ackrell, B. A.; Kearney, E. B.; Singer, T. P. Mammalian succinate dehydrogenase. *Methods Enzymol.* **1978**, *53*, 466−483.

(20) Bamford, V.; Dobbin, P. S.; Richardson, D. J.; Hemmings, A. M. Open conformation of a flavocytochrome c3 fumarate reductase. *Nat. Struct. Biol.* **1999**, *6*, 1104−1107.

(21) Taylor, P.; Pealing, S. L.; Reid, G. A.; Chapman, S. K.; Walkinshaw, M. D. Structural and mechanistic mapping of a unique fumarate reductase. *Nat. Struct. Biol.* **1999**, *6*, 1108−1112.

(22) Doherty, M. K.; Pealing, S. L.; Miles, C. S.; Moysey, R.; Taylor, P.; Walkinshaw, M. D.; Reid, G. A.; Chapman, S. K. Identification of the Active Site Acid/Base Catalyst in a Bacterial Fumarate Reductase: A Kinetic and Crystallographic Study. *Biochemistry* **2000**, *39*, 10695−10701.

(23) Leys, D.; Tsapin, A. S.; Nealson, K. H.; Meyer, T. E.; Cusanovich, M. A.; Van Beeumen, J. J. Structure and mechanism of the flavocytochrome c fumarate reductase of Shewanella putrefaciens MR-1. *Nat. Struct. Biol.* **1999**, *6*, 1113−1117.

(24) Quastel, J. H.; Whetham, M. D. The equilibria existing between succinic, fumaric, and malic acids in the presence of resting bacteria. *Biochem. J.* **1924**, *18*, 519−534.

(25) Massey, V.; Singer, T. P. Studies on succinic dehydrogenase. III The fumaric reductase activity of succinic dehydrogenase. *J. Biol. Chem.* **1957**, *228*, 263−274.

(26) Warringa, M. G. P. J.; Smith, O. H.; Giuditta, A.; Singer, T. P. Studies on succinic dehydrogenase. VIII Isolation of a succinic dehydrogenase-fumaric reductase from an obligate anaerobe. *J. Biol. Chem.* **1958**, *230*, 97−109.

(27) Grivennikova, V. G.; Gavrikova, E. V.; Timoshin, A. A.; Vinogradov, A. D. Fumarate reductase activity of bovine heart succinate-ubiquinone reductase. New assay system and overall properties of the reaction. *Biochim. Biophys. Acta* **1993**, *1140*, 282−292.

(28) Hirst, J.; Sucheta, A.; Ackrell, B. A. C.; Armstrong, F. A. Electrocatalytic voltammetry of succinate dehydrogenase: direct quantification of the catalytic properties of a complex electron-transport enzyme. *J. Am. Chem. Soc.* **1996**, *118*, 5031−5038.

(29) Iverson, T. M.; Luna-Chavez, C.; Croal, L. R.; Cecchini, G.; Rees, D. C. Crystallographic studies of the Escherichia coli quinol-fumarate reductase with inhibitors bound to the quinol-binding site. *J. Biol. Chem.* **2002**, *277* (18), 16124−16130.

(30) Yankovskaya, V.; Horsefield, R.; Törnroth, S.; Luna-Chavez, C.; Miyoshi, H.; Léger, C.; Byrne, B.; Cecchini, G.; Iwatam, S. Architecture of Succinate Dehydrogenase and Reactive Oxygen Species Generation. *Science* **2003**, *299* (5607), 700−704.

(31) Lancaster, C. R. D.; Gross, R.; Simon, J. A third crystal form of Wolinella succinogenes quinol:fumarate reductase reveals domain closure at the site of fumarate reduction. *Eur. J. Biochem.* **2001**, *268*, 1820−1827.

(32) Gest, H. The evolution of biological energy-transducing systems. *FEMS Microbiol. Lett.* **1980**, *7*, 73−77.

(33) Wood, D.; Darlison, M. G.; Wilde, R. J.; Guest, J. R. Nucleotide sequence encoding the flavoprotein and hydrophobic subunits of the succinate dehydrogenase of Escherichia coli. *Biochem. J.* **1984**, *222*, 519−534.

(34) Walker, W. H.; Singer, T. P. Identification of the covalently bound flavin of succinate dehydrogenase as 8-alpha-(histidyl) flavin adenine dinucleotide. *J. Biol. Chem.* **1970**, *245* (16), 4224−4225.

(35) Blaut, M.; Whittaker, K.; Valdovinos, A.; Ackrell, B. A.; Gunsalus, R. P.; Cecchini, G. Fumarate reductase mutants of Escherichia coli that lack covalently bound flavin. *J. Biol. Chem.* **1989**, *264* (23), 13599−13604.

(36) Robinson, K. M.; Rothery, R. A.; Weiner, J. H.; Lemire, B. D. The covalent attachment of FAD to the flavoprotein of Saccharomyces cerevisiae succinate dehydrogenase is not necessary for import and assembly into mitochondria. *Eur. J. Biochem.* **1994**, *222*, 983−990.

(37) Morris, C. J.; Black, A. C.; Pealing, S. L.; Manson, F. D.; Chapman, S. K.; Reid, G. A.; Gibson, D. M.; Ward, F. B. Purification and properties of a novel cytochrome: flavocytochrome c from Shewanella putrefaciens. *Biochem. J.* **1994**, *302*, 587−593.

(38) Turner, K. L.; Doherty, M. K.; Heering, H. A.; Armstrong, F. A.; Reid, G. A.; Chapman, S. K. Redox properties of flavocytochrome c3 from Shewanella frigidimarina NCIMB400. *Biochemistry* **1999**, *38*, 3302−3309.

(39) Mowat, C.; Moysey, R.; Miles, C.; Leys, D.; Doherty, M.; Taylor, P.; Walkinshaw, M.; Reid, G.; Chapman, S. K. Kinetic and Crystallographic Analysis of the Key Active Site Acid/Base Arginine in a Soluble Fumarate Reductase. *Biochemistry* **2001**, *40*, 12292−12298.

(40) Pankhurst, K.; Mowat, C.; Miles, C.; Leys, D.; Walkinshaw, M.; Reid, G.; Chapman S. Role of His505 in the Soluble Fumarate Reductase from Shewanella frigidimarina. *Biochemistry* **2002**, *41*, 8551−8556.

(41) Vik, S. B.; Hatefi, Y. Possible occurrence and role of an essential histidyl residue in succinate dehydrogenase. *Proc. Natl. Acad. Sci. U.S.A.* **1981**, *78* (11), 6749−6753.

(42) Mowat, C.; Pankhurst, K.; Moysey, R.; Miles, C.; Leys, D.; Walkinshaw, M.; Reid, G.; Chapman, S. K. Engineering water to act as an active site acid catalyst in a soluble fumarate reductase. *Biochemistry* **2002**, *41*, 11990−11996.

(43) Frisch, M. J.; Trucks, G. W.; Schlegel, H. B.; Scuseria, G. E.; Robb, M. A.; Cheeseman, J. R.; Montgomery, J. A., Jr.; Vreven, T.; Kudin, K. N.; Burant, J. C.; Millam, J. M.; Iyengar, S. S.; Tomasi, J.; Barone, V.; Mennucci, B.; Cossi, M.; Scalmani, G.; Rega, N.; Petersson, G. A.; Nakatsuji, H.; Hada, M.; Ehara, M.; Toyota, K.; Fukuda, R.; Hasegawa, J.; Ishida, M.; Nakajima, T.; Honda, Y.; Kitao, O.; Nakai, H.; Klene, M.; Li, X.; Knox, J. E.; Hratchian, H. P.; Cross, J. B.; Bakken, V.; Adamo, C.; Jaramillo, J.; Gomperts, R.; Stratmann, R. E.; Yazyev, O.; Austin, A. J.; Cammi, R.; Pomelli, C.; Ochterski, J. W.; Ayala, P. Y.; Morokuma, K.; Voth, G. A.; Salvador, P.; Dannenberg, J. J.; Zakrzewski, V. G.; Dapprich, S.; Daniels, A. D.; Strain, M. C.; Farkas, O.; Malick, D. K.; Rabuck, A. D.; Raghavachari, K.; Foresman, J. B.; Ortiz, J. V.; Cui, Q.; Baboul, A. G.; Clifford, S.; Cioslowski, J.; Stefanov, B. B.; Liu, G.; Liashenko, A.; Piskorz, P.; Komaromi, I.; Martin, R. L.; Fox, D. J.; Keith, T.; Al-Laham, M. A.; Peng, C. Y.; Nanayakkara, A.; Challacombe, M.; Gill, P. M. W.; Johnson, B.; Chen, W.; Wong, M. W.; Gonzalez, C.; Pople, J. A. *Gaussian03*, revision C.02; Gaussian, Inc.: Wallingford, CT, 2004.

(44) Becke, A. D. Completely numerical calculations on diatomic molecules in the local-density approximation. *Phys. Rev. A* **1986**, *33* (4), 2786−2788.

(45) Becke, A. D. Density-functional exchange-energy approximation with correct asymptotic behavior. *Phys. Rev. A* **1988**, *38* (6), 3098−3100.

(46) Becke, A. D. A New Mixing of Hartree-Fock and Local Density-Functional Theories. *J. Chem. Phys.* **1993**, *98*, 1372−1377.

(47) Becke, A. D. Density-Functional Thermochemistry. 3. The Role of Exact Exchange. *J. Chem. Phys.* **1993**, *98*, 5648−5652.

(48) Lee, C.; Yang, W.; Parr, R. G. Development of the Colle-Salvetti correlation-energy formula into a functional of the electron density. *Phys. Rev. B* **1988**, *37*, 785−789.

(49) Fernandes, P. A.; Ramos, M. J. Theoretical Insights into the Mechanism for Thiol/Disulfide Exchange. *Chem.*−Eur. J. **2003**, *10* (1), 257−266.

(50) Lucas, M. F.; Ramos, M. J. A theoretical study of the suicide inhibition mechanism of the enzyme Pyruvate Formate Lyase by methacrylate. *J. Am. Chem. Soc.* **2005**, *127* (18), 6902−6909.

(51) Prabhakar, R.; Siegbahn, P. E. M. A Theoretical Study of the Mechanism for the Reductive Half-Reaction of Pea Seedling Amine Oxidase (PSAO). *J. Phys. Chem. B* **2001**, *105*, 4400−4408.

(52) K.-B. Cho, H.; Gräslund, F. A.; Siegbahn, P. E. M. The Substrate Reaction Mechanism of Class III Anaerobic Ribonucleotide Reductase. *J. Phys. Chem. B* **2001**, *105*, 6445−6452.

(53) Himo, F.; Siegbahn, P. E. M. Catalytic Mechanism of Glyoxalase I: A Theoretical Study. *J. Am. Chem. Soc.* **2001**, *123*, 10280−10289.

(54) Pelmenschikov, V.; Blomberg, M. R. A.; Siegbahn, P. E. M. A theoretical study of the mechanism for peptide hydrolysis by thermolysin. *J. Biol. Inorg. Chem.* **2002**, *7*, 284−298.

(55) Torres, R. A.; Himo, F.; Bruice, T. C.; Noodleman, L.; Lovell, T. Theoretical Examination of Mg2+-Mediated Hydrolysis of a Phosphodiester Linkage as Proposed for the Hammerhead Ribozyme. *J. Am. Chem. Soc.* **2003**, *125* (32), 9861−9867.

(56) Barone, V.; Cossi, M.; Tomasi, J. A new definition of cavities for the computation of solvation free energies by the polarizable continuum model. *J. Chem. Phys.* **1997**, *107*, 3210−3221.

(57) Cossi, M.; Barone, V.; Robb, M. A. A direct procedure for the evaluation of solvent effects in MC-SCF calculations. *J. Chem. Phys* **1999**, *111* (12), 5295−5302.

(58) Cossi, M.; Barone, V. Solvent effect on vertical electronic transitions by the polarizable continuum model. *J. Chem. Phys.* **2000**, *112*, 242724-35.

(59) Cossi, M.; Rega, N.; Scalmani, G.; Barone, V. Energies, structures, and electronic properties of molecules in solution with the C-PCM solvation model. *J. Comput Chem.* **2003**, *24* (6), 669−681.

(60) Miertus, S.; Scrocco, E.; Tomasi, J. Electrostatic Interaction of a Solute with a Continuum. A Direct Utilization of ab initio Molecular Potentials for the Provision of Solvent Effects. *Chem. Phys.* **1981**, *55*, 117.

(61) Tomasi, S. M. a. J. Approximate Evaluations of the Electrostatic Free Energy and Internal Energy Changes in Solution Processes. *Chem. Phys.* **1982**, *65*, 239.

(62) Cossi, M.; Scalmani, G.; Rega, N.; Barone, V. New developments in the polarizable continuum model for quantum mechanical and classical calculations on molecules in solution. *J. Chem. Phys.* **2002**, *117*, 43−54.

(63) Tomasi, J.; Bonaccorsi, R. Methodological aspects of the solvation models based on continuous solvent distributions. *Croat. Chem. Acta* **1992**, *65*, 29−54.

(64) Blomberg, M. R. A.; Siegbahn, P. E. M.; Babcock, G. T. Modeling Electron Transfer in Biochemistry: A Quantum Chemical Study of Charge Separation in Rhodobacter sphaeroides and Photosystem II. *J. Am. Chem. Soc.* **1998**, *120*, 8812−8824.

(65) Siegbahn, P. E. M.; Eriksson, L.; Himo, F.; Pavlov, M. Hydrogen Atom Transfer in Ribonucleotide Reductase (RNR). *J. Phys. Chem. B* **1998**, *102* (51), 10622−10629.

(66) Pereira, S.; Fernandes, P. A.; Ramos, M. J. Theoretical Study on the Inhibition of Ribonucleotide Reductase by 2′-Mercapto-2′-deoxyribonucleoside-5′-diphosphates. *J. Am. Chem. Soc.* **2005**, *127* (14), 5174−5179.

(67) Lucas, M. F.; Fernandes, P. A.; Eriksson, L. A.; Ramos, M. J. Pyruvate Formate Lyase: A New Perspective. *J. Phys. Chem. B* **2003**, *107*, 5751−5757.

(68) Himo, F.; Eriksson, L. A. Catalytic Mechanism of Pyruvate Formate-Lyase; A Theoretical Study. *J. Am. Chem. Soc.* **1998**, *120*, 11449−11455.

(69) Siegbahn, P. E. M. A Theoretical Study of the Substrate Mechanism of Ribonucleotide Reductase. *J. Am. Chem. Soc.* **1998**, *120*, 8417−8429.

(70) Siegbahn, P. E. M. Two, Three and Four Water Chain Models for the Nucleophilic Addition Step in the Wacker Process. *J. Phys. Chem.* **1996**, *100*, 14672−14680.